Tetrahedron 65 (2009) 4298–4303

Contents lists available at ScienceDirect

Tetrahedron

journal homepage: www.elsevier.com/locate/tet

Polyglycerol-bound phosphotriesterase enzyme model complexes for detection and hydrolysis of phosphorus species in aqueous solution

Anshuman Mangalum, Rhett C. Smith *

Department of Chemistry and Center for Optical Materials Science and Engineering Technologies (COMSET), Clemson University, Clemson, SC 29634, USA

ARTICLE INFO

Article history:
Received 22 October 2008
Received in revised form 17 March 2009
Accepted 19 March 2009
Available online 27 March 2009

Keywords:
Hyperbranched polymer
Phosphohydrolase
Pyrophosphate sensor

ABSTRACT

Phosphotriesterase models incorporating di(2-picolyl)amino ligands supported by *m*-xylylene or 2-hydroxy-*m*-xylylene scaffolds have been tethered to the periphery of a water-soluble hyperbranched polyglycerol (PG). In aqueous solution buffered at pH 7.4, the polymeric complexes of Zn^{2+} are useful receptors for polymeric indicator displacement assays for phosphate and pyrophosphate employing commercial complexometric indicators. Under the same conditions, the Co^{3+} effectively hydrolyze *p*-nitrophenylphosphate with approximately five orders of magnitude rate enhancement versus uncatalyzed hydrolysis. These systems offer promising results as mixed-metal dual detect-decontaminate materials for organophosphorus toxins under mild, neutral aqueous conditions.

1. Introduction

The nerve agents of chemical warfare, as well as many widely used commercial pesticides, are phosphoesters. Some of these neurotoxic compounds, including G and V agents (Chart 1) are among the most toxic synthetic materials ever isolated. The simple structure and availability of starting materials make these agents attractive weapons for terrorism, as exemplified by the use of sarin (GB) in attacks on subway trains in Japan in 1995.[1] Recent increases in awareness regarding terrorist threats and the environmental impact of pesticides highlight the desire to detect[2,3] and degrade[4,5] organophosphorus toxins. Phosphotriesterase (PTEase) is a bacterial dizinc hydrolase enzyme capable of hydrolyzing phosphoesters.[6] The active site of PTEase features two zinc ions held at a distance of ~3.4 Å.[7] One actively explored area of research is thus to prepare small molecule bimetallic models of PTEase that can catalytically hydrolyze phosphoesters to biologically innocuous phosphates. Di(2-picolylaminomethyl)xylyl scaffolded ligands of the general form shown in Chart 2 support dizinc complexes with M–M distances similar to that in the native PTEase active site. Complexes of such ligands have thus been utilized in a variety of sensing and catalytic applications under physiological conditions.[8–17] An IR-dye modified variation has been applied to image phosphate production resulting from bacterial infection in live mice, unequivocally demonstrating the stability of this binucleating scaffold for extended periods in biological milieu.[18] Our work with PTEase model-based detection[8] has focused on the indicator displacement assay sensing mechanism.[19] In this

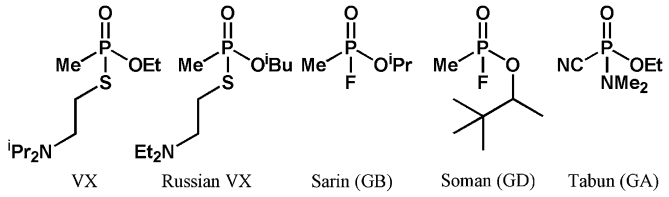

Chart 1. Five of the seven globally stockpiled chemical warfare agents are simple phosphoesters.

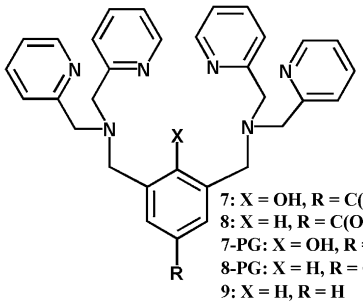

7: X = OH, R = C(O)OH
8: X = H, R = C(O)OH
7-PG: X = OH, R = C(O)O-polyglycerol
8-PG: X = H, R = C(O)O-polyglycerol
9: X = H, R = H
10: X = OH, R = CH_3

Chart 2. General form of binucleating ligands whose bimetallic complexes are useful for inorganic phosphate detection and can catalytically hydrolyze phosphoesters.

* Corresponding author. Tel.: +1 864 656 6112; fax: +1 864 656 6613.
E-mail address: rhett@clemson.edu (R.C. Smith).

0040-4020/$ – see front matter © 2009 Elsevier Ltd. All rights reserved.
doi:10.1016/j.tet.2009.03.051

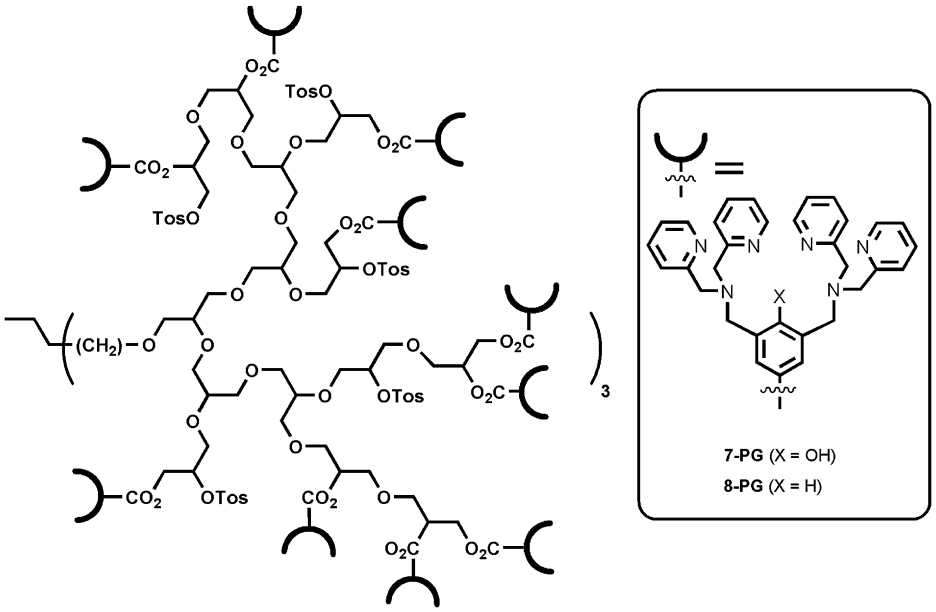

Chart 3. Representation of the structure of **7–PG** and **8–PG**. Note that the size of PG branches varies, and this is only one possible representation demonstrating the global structure of the PG.

strategy an optical (colorimetric or fluorescent) signal transduction event is effected by displacement of an indicator from a receptor upon exposure to an analyte. Sensitivity is attained when the analyte binds significantly more strongly to the receptor than does the displaceable indicator. This strategy is attractive because a variety of commercial indicators can be utilized, providing various response wavelengths and binding affinities with a single receptor, and the simple visual colorimetric detection provided by this strategy is desirable for field use. Related bioorganic model-based indicator displacement assays for nerve agents operate via metal ion displacement from fluorogenic ligands in response to neutral nerve agent simulants[20] or anionic partial hydrolysis products of G agents.[21]

Another of our interests is to tether PTEase models to polymeric supports for catalytic applications. Covalent linkage or physical encapsulation of native phosphohydrolase enzymes to polymers and foams has already shown promise for decontamination.[22,23] Covalent linkage is preferred because it prevents catalyst leaching from the polymer, thus increasing shelf life of the material. Model complexes should be an affordable alternative to isolated enzymes and may be more robust components of decontamination solutions. The polymer support we selected for this initial study is a biocompatible water-soluble hyberbranched polyglycerol (Chart 3).

In selecting a polymer support for a decontamination catalyst, biocompatibility and high surface area for functionalization are advantageous. Dendrimers are promising chaperones for drug targeting/delivery and their high surface area and potential for supporting cooperative effects have been exploited for catalytic applications.[24–27] The often time-consuming synthesis of dendrimers, however, is the most auspicious hindrance to their widespread application. Hyperbranched polymers, however, can be prepared more efficiently and retain the high surface area typical of dendrimers.[28–30] Biocompatible hyperbranched polymers are thus privileged scaffolds for high activity bioremediation and decontamination technologies. For organophosphorus neurotoxins, polymers such as polyglycerol, which can efficiently permeate and solubilize agents from thickened chemical agent mixtures often used in warfare contexts (where poly(ethylene glycol) is a preferred thickener),[31] are of particular relevance in a practical sense.[4] Polyglycerol is approved in the United States and Europe for use in pharmaceuticals,[32–34] cosmetics,[35,36] and even as food additives,[37,38] making it a safe candidate for protective creams. The bioavailability of polyglycerol[32,33] also suggests its potential as a carrier support to deliver OP-decontaminating agents in prophylactic medical treatment. A polymeric support also facilitates catalyst recyclability and use in continuous membrane reactors for water treatment.

Herein we describe the preparation of hyperbranched polyglycerol modified by two dinucleating PTE model ligand scaffolds. We demonstrate that their Co(III) complexes efficiently hydrolyze a phosphoester model compound, and that their Zn(II) complexes are useful receptors for indicator displacement assays for phosphate/pyrophosphate. Both hydrolysis and detection experiments were carried out under ambient conditions in aqueous solution buffered at physiological pH (7.4).

2. Results and discussion

The hyperbranched PG support (M_n=3700, PDI=1.2) was prepared via a literature protocol[39] involving anionic polymerization of glycidol from a trimethylolpropane core. In order to facilitate attachment of PTE models, the PG was reacted with tosyl chloride in the presence of pyridine to give tosylated polyglycerol (**Tos–PG**).[40] The small molecules carboxylate-derivatized binucleating ligand moieties required for condensation with **Tos–PG** were readily prepared via the sequence shown in Scheme 1. Simple S_N2 reaction of **PG–Tos** with deprotonated **7** or **8** yields **7–PG** and **8–PG**, respectively (Chart 3; the size of PG branches will vary and the structure shown is a simplified representation). The approach selected to tether enzyme model complexes to the polymers was inspired by a reported route to hyperbranched PGs derivatized with α,α′-diamino-*m*-xylene-based pincer ligands in which highly efficient complex loading was accomplished, leading to active complexes for Pd-catalyzed C–C bond forming reactions.[40–42] In the current system, the efficiency of substituting **7** or **8** for tosylate units was readily gauged by integration of well-resolved ^{1}H NMR resonances at ~2.3 ppm (tosyl methyl group) and ~8.5 ppm (pyridyl subunit). Unfortunately, a relatively low loading efficiency (36% and 25% of tosyl groups substituted in **7–PG** and **8–PG**, respectively) was observed, despite repeated efforts to improve this step. The low efficiency is presumably a result of the fairly

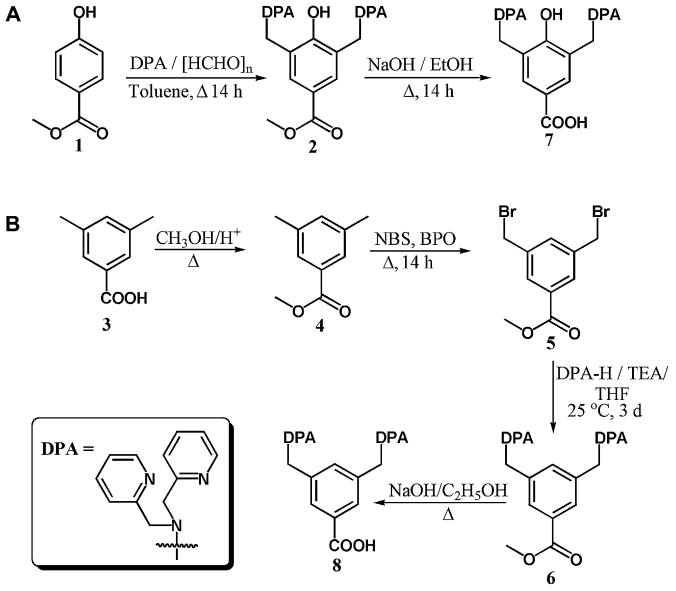

Scheme 1. Preparation of **7** (A) and **8** (B).

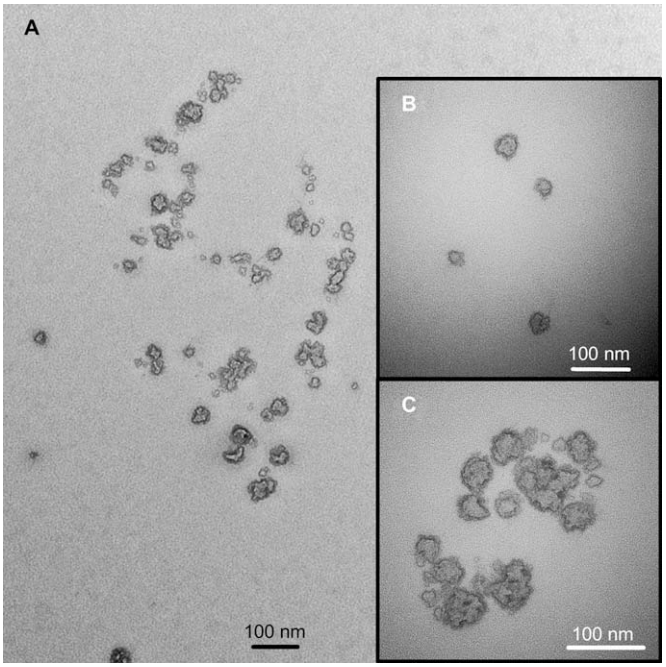

Figure 1. TEM image of **8–PG** (A). Insets show a set of variously sized particles (B) and an agglomeration of smaller particles that make up larger features (C).

voluminous carboxylates lacking sufficient access to some potential substitution sites due to crowding by the hyperbranched support.

The Zn_2–**8–PG** metal complex was readily prepared by dissolving **8–PG** with 2 equiv of $Zn(ClO_4)_2 \cdot 6H_2O$ in 0.1 M HEPES buffer (pH 7.4). Upon dispersion in a solvent such as THF, hyperbranched polyglycerol-supported transition metal complexes have been shown to form micellar structures that can be fractionated by size exclusion chromatography to produce uniformly sized nanostructures.[40] Although preparing nanostructures is not the primary goal of the current study, we were interested in whether **7** and **8** form structures similar to those reported previously. We thus conducted a transmission electron microscopy (TEM) study on a sample cast from a (nonfractionated) dispersion of **8–PG** in THF. The TEM images of the Zn_2–**8–PG** complex (i.e., Fig. 1) revealed that irregularly shaped particles, similar in size to those previously reported,[40] were observed. The particles ranged in size from about 15 to 35 nm (Fig. 1B), and close inspection reveals that the apparent larger features visible in Figure 1A are actually clusters of the smaller particles (Fig. 1C). The formation of micellar or reverse micellar nanostructures is of particular interest because catalysis can be enhanced within micellar structures or at their surface, depending on the substrate and solvent system employed. Catalyst recovery could also be affected by nanofiltration, ultracentrifugation or membrane techniques for particles in this size regime. These avenues are worth pursuing in more detail once optimized materials are accomplished.

In order to test the viability of the PG-supported complexes to hydrolyze phosphoesters, the hydrolysis rate of 4-nitrophenylphosphate (NPP) was examined in the presence of **7–PG** and **8–PG** Co(III) complexes. NPP is a convenient and often-used substrate for such studies because the formation of its hydrolysis product, 4-nitrophenolate, is easily followed by UV–vis spectroscopy.[43,44] By following NPP hydrolysis by absorption spectroscopy, employing solutions with varying substrate and catalyst concentrations as previously reported,[44] we determined the rate constants for NPP hydrolysis in HEPES (0.1 M, pH=7.4) with the Co(III) complexes of **7–PG** ($4.8\times10^{-4}\ s^{-1}$) and **8–PG** ($6.2\times10^{-4}\ s^{-1}$). These values indicate an approximate five orders of magnitude enhancement in hydrolysis rate for either of the PG-bound Co(III) complexes versus the uncatalyzed hydrolysis rate of $2\times10^{-9}\ s^{-1}$.[45] Although higher activity would likely be necessary for practical application requiring hydrolysis of more challenging substrates, these preliminary complexes show promise for extension to additional polymer-bound complexes. The ready water solubility of the polyglycerol-bound derivatives and the facile separation from a vessel of water by dialysis offer improved practical utility of the materials versus small molecular analogues.

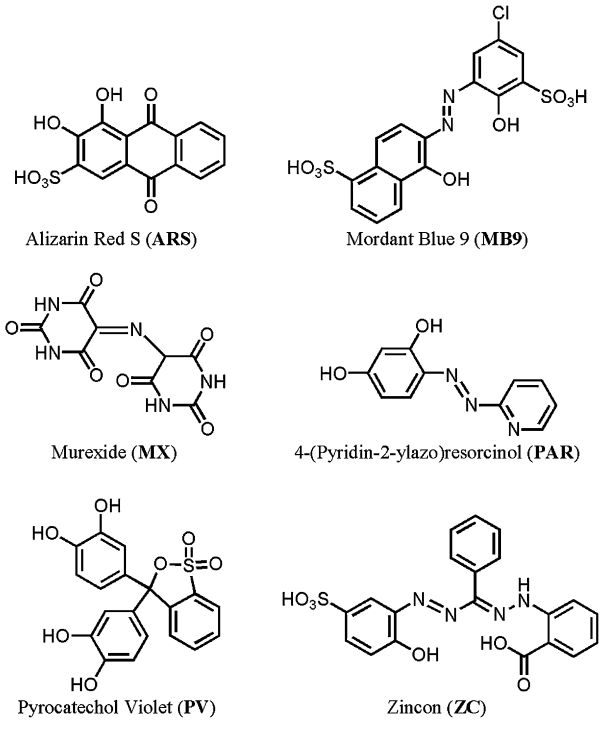

Chart 4. Structures of commercially available complexometric indicators used in the current study. Only one protonation state/resonance structure is shown in each case.

Another interesting application of polymer-bound enzyme models is their ability to act as selective receptors for the detection of biological species. In this case, the Zn(II) complexes (Zn_2–**7–PG** and Zn_2–**8–PG**) were employed rather than the Co(III) complexes used in hydrolysis studies, because Zn(II) has greater ligand lability and thus favors reversible binding that is desirable for sensors. Building on our work with related dizinc complexes,[8] we tested the polymer-bound analogues as macromolecular receptors in indicator displacement assays (IDAs) for inorganic phosphate detection. The first step in this direction was to determine how Zn_2–**8–PG** complexes influence the absorption spectra of commercially available complexometric indicators upon binding, and whether the indicators are successfully displaced by various analytes. A large color change between the complex-bound and free (analyte-displaced) indicator states is desired because this would facilitate detection of small quantities of analyte.

On the basis of our previous study,[8] we selected six dyes (Chart 4) as indicators capable of potentially large color changes. As an example of how dramatically spectral properties can change upon complexation, data from a titration of **MX** with Zn_2–**8–PG** and subsequent displacement of the indicator by addition of pyrophosphate are shown in Figure 2 (similar data for the remaining dyes are provided in Supplementary data). Data from absorption spectroscopic titrations were used to extract dissociation constants (K_d) for the indicators (Table 1). Table 1 also provides K_d values for the indicators with dizinc complexes of nonpolymer-bound ligands **9** and **10** (Chart 2) for comparison. Because the polymer-bound variations are in significantly altered environments in terms of both polarity and sterics, it is not surprising that there is a marked change in the dissociation constants for indicators bound to Zn_2–**7–PG** or Zn_2–**8–PG** complexes versus the small molecule analogues.

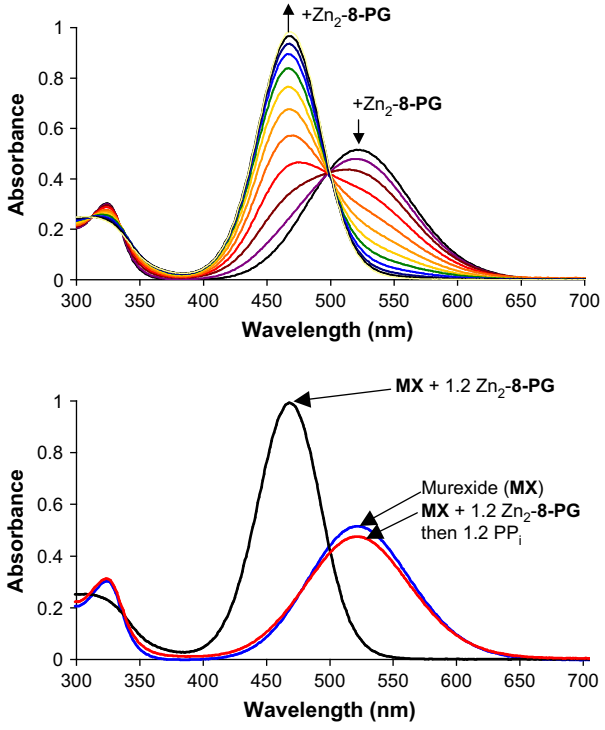

Figure 2. Upper chart: changes in absorption spectra of murexide (5.0×10^{-5} M) as up to 1 equiv of Zn_2–**8–PG** is added to the solution. The first trace is murexide alone, and each subsequent trace represents addition of 0.1 equiv of Zn_2–**8–PG**. Lower chart: absorption spectra for murexide alone (blue trace), the same solution immediately after addition of 1.2 equiv Zn_2–**8–PG** (black trace), and subsequently 1.2 equiv pyrophosphate (PP_i, red trace). All solutions were in 0.1 M HEPES buffer at a pH of 7.4. Spectra are corrected for dilution factors.

Table 1
Dissociation constants (K_d, in μM) for the binding of indicators to the dizinc complexes of the listed ligands, determined from absorption spectroscopic data (in 0.1 M HEPES buffer at pH 7.4). Structures and abbreviations for indicators are provided in Chart 4, and absorption spectra are provided in Supplementary data

Dissociation constants (K_d, μM)				
Indicator	**8–PG**	**7–PG**	**9**	**10**
ARS	60	42	63	280
MB9	NA[a]	29	NA[a]	5.1
MX	83	350	640	21
PAR	3.4	48	28	18
PV	110	160	98	30
ZC	68	59	480	2.9

[a] Spectroscopic data could not be adequately fit using this model.

These changes in binding constant are accompanied by concomitant changes in how effectively inorganic phosphate anions displace the indicators to produce colorimetric responses. Though *m*-xylylene-supported bis(di(2-picolylamine)) dizinc complexes are useful phosphate (P_i) sensors,[9–16] there is some evidence that pyrophosphate (PP_i) can bind more strongly, at least in some cases.[8,46] Furthermore, selectivity can be acquired simply by judicious selection of the indicator to be displaced by the analyte (i.e., by selecting an indicator with an appropriate K_d).[46] The polymer-bound analogues behave similarly: when the dizinc complex is the receptor, *any* of the indicators shown in Chart 4 are selective for inorganic phosphates (P_i or PP_i) over all other common anions screened. No notable change in absorbance was observed in response to F^-, Cl^-, Br^-, I^-, AcO^- or HSO_4^- (all in 0.1 M HEPES, pH=7.4). An even greater specificity can be attained when the most weakly binding indicators are employed. Specifically, we found that PP_i can be selectively detected versus P_i at the same concentration when **MX** or **PV** is used as the indicator (The response using **MX** is shown in Fig. 2; other absorption spectra are shown in Supplementary data.). It is noteworthy that the best receptor–indicator pairs for the polyglycerol differ from those for small molecule analogues,[8] emphasizing the importance of independent K_d measurements and indicator displacement trials in the course of polymer-bound sensor development.

3. Conclusions

We have prepared artificial enzyme modified, water-soluble hyperbranched polyglycerols. The Co(III) complexes of these materials catalyze the hydrolysis of a phosphoester model substrate in neutral aqueous buffer, with a rate enhancement of five orders of magnitude versus the uncatalyzed reaction. Zinc(II) complexes of PG-bound enzyme models are highly selective receptors for inorganic phosphates over other common anions. There are significant differences in binding constants between the polyglycerol-supported enzyme models and their small molecule analogues. Caution should thus be exercised when attempting to extend data from small molecule model systems to polymer-bound analogues, especially in IDA studies where relative binding strengths dictate the selectivity of the receptor–indicator pairs for a given analyte. Additional polymer supported PTEase model-derivatized hyperbranched polymers are currently being prepared for optimization in our laboratory to improve upon the strategies reported herein.

4. Experimental

4.1. Materials and characterization methods

All reagents were obtained from Aldrich Chemical Co., TCI America, Alfa Aesar, Mallinckrodt, or MP Biomedicals, LLC and used

as received. Hyperbranched polyglycerol[39] and tosylated polyglycerol[40] were prepared as previously described. NMR spectra were recorded on a Bruker Avance 300 spectrometer and chemical shifts are reported in parts per million (δ ppm). Proton NMR was internally referenced to tetramethylsilane (δ 0.0) or residual solvent signal; ^{13}C NMR chemical shifts were reported relative to the residual solvent peak. TEM imaging was performed using a Hitachi H-7600 variable kV TEM with acceleration voltage of 120 kV. The sample was prepared on formwar coated copper grids by drop-casting, and samples were dried in an oven overnight. Compounds **4** and **5** were prepared as previously reported.[47]

4.2. Synthesis

*4.2.1. Methyl 3,5-bis[(bis(2-pyridylmethyl)amino)methyl]-benzoate (**6**)*

A solution of **5** (1.0 g, 3.1 mmol) in 5 mL of anhydrous THF was stirred at 0 °C under inert nitrogen atmosphere. In another vial, a solution of triethylamine (1.3 g, 12.9 mmol) and DPA (1.3 g, 6.5 mmol) was prepared and then added dropwise to the solution of **5**. The reaction was allowed to warm at room temperature after complete addition and the reaction mixture was stirred for 3 days. The triethylammonium bromide was filtered off and volatiles were removed under reduced pressure, leaving behind a red oil. Dichloromethane (50 mL) was added and solution was washed with saturated Na_2CO_3 (aq) (3×50 mL). The organic layer was collected and dried over Na_2SO_4, then volatiles were removed under reduced pressure, yielding a viscous red oil (1.3 g, 72.0%). ^{1}H NMR (300 MHz, $CDCl_3$): δ=3.74 (s, 4H, C–CH_2), 3.82 (s, 8H, N–CH_2), 3.93 (s, 3H, OCH_3), 7.15 (br, 4H, pyridyl), 7.6 (m, 8H, pryidyl), 7.75 (s, 1H, aromatic), 7.95 (d, 2H, J=1.5, aromatic), 8.52 (m, 4H, pryidyl). ^{13}C NMR (75.4 MHz, $CDCl_3$): δ=58.2, 60.1, 67.9, 122.0, 122.8, 128.8, 130.2, 133.8, 136.5, 139.7, 148.9, 159.5, 167.2. HRMS (FAB, m/z): calcd for $C_{34}H_{34}N_6O_2$ 558.2743; found 558.2749. This material was hydrolyzed to form the acid without further purification.

*4.2.2. 3,5-Bis[(bis(2-pyridylmethyl)amino)methyl]-benzoic acid (**8**)*

Compound **6** (1.3 g, 2.2 mmol) was dissolved in 60 mL of ethanol and ~1.2 g of NaOH was added into the reaction mixture. After addition, the solution was refluxed overnight. Volatiles were removed by rotary evaporation, then water was added to the residue and extracted with dichloromethane (3×30 mL). The organic layer was dried over Na_2SO_4, and volatiles were removed under reduced pressure to give a yellow solid (0.09 g, 7.00%). ^{1}H NMR (300 MHz, $CDCl_3$): δ=3.32 (s, 4H, C–CH_2), 3.52 (s, 8H, N–CH_2), 6.84 (t, 4H, J=6.0, pyridyl), 7.19–7.38 (m, 8H, pryidyl), 7.79 (s, 2H, aromatic), 8.38 (d, 4H, J=4.5, pryidyl). ^{13}C NMR (75.4 MHz, $CDCl_3$): δ=58.9, 59.9, 121.9, 122.9, 129.3, 131.0, 136.4, 137.4, 138.3, 149.0, 159.2, 173.8. HRMS (FAB, m/z): calcd for $C_{33}H_{33}N_6O_2$ 545.2665; found 545.2674.

*4.2.3. Methyl 3,5-bis[(bis(2-pyridylmethyl)amino)methyl]-4-hydroxybenzoate (**2**)*

Compound **1** (1.0 g, 6.6 mmol) was taken in a round bottom flask. DPA (3.9 g, 19.6 mmol), paraformaldehyde (0.6 g, 20.0 mmol), and 40 mL toluene were then added. After addition, the reaction mixture was refluxed overnight. After cooling to room temperature, toluene was removed under reduced pressure and the residue was dissolved in CH_2Cl_2. The resultant solution was washed with saturated Na_2CO_3 (4×50 mL). The organics were dried over Na_2SO_4 and then volatiles were removed by rotary evaporation. The desired product was obtained as a viscous red oil (2.6 g, 69.0%). ^{1}H NMR (300 MHz, $CDCl_3$): δ=3.85 (s, 4H, C–CH_2), 3.90 (s, 11H, N–CH_2 and OCH_3), 7.15 (m, 4H, pyridyl), 7.50 (d, 4H, J=7.8 Hz, pryidyl), 7.65 (m, 4H, pryidyl), 7.95 (s, 2H, aromatic), 8.55 (dd, ^1J=6.0 Hz, ^2J=0.9 Hz, 4H, pryidyl). ^{13}C NMR (75.4 MHz, $CDCl_3$): δ=51.7, 54.5, 59.7, 120.1, 122.0, 122.9, 124.4, 131.1, 136.6, 148.8, 159.1, 160.7, 167.3. HRMS (FAB, m/z): calcd for $C_{34}H_{34}N_6O_3$ 574.2692; found 574.2700. This material was hydrolyzed to form the acid without further purification.

*4.2.4. 3,5-Bis[(bis(2-pyridylmethyl)amino)methyl]-4-hydroxybenzoic acid (**7**)*

Compound **2** (0.2 g, 0.3 mmol) was dissolved in 10 mL of ethanol and ~1.2 g of NaOH was added into the reaction mixture. After addition, solution was refluxed overnight. Volatiles were removed by rotary evaporation and water was added into the residue and solution was extracted with dichloromethane (3×30 mL). The organic layer was dried over Na_2SO_4, filtered, and volatiles were removed under reduced pressure (0.09 g, 26.30%). ^{1}H NMR (300 MHz, $CDCl_3$): δ=3.85 (s, 4H, C–CH_2), 3.95 (s, 8H, N–CH_2), 7.15 (m, 4H, pyridyl), 7.52 (d, 4H, J=7.8 Hz, pryidyl), 7.65 (m, 4H, pryidyl), 8.10 (s, 2H, aromatic), 8.55 (d, 4H, J=4.2 Hz, pryidyl). ^{13}C NMR (75.4 MHz, $CDCl_3$): δ=59.3, 63.0, 121.1, 122.7, 123.0, 124.3, 131.0, 137.1, 149.1, 158.9, 160.3, 167.8. HRMS (FAB, m/z): calcd for $C_{33}H_{33}N_6O_3$ 561.2614; found 561.2623.

*4.2.5. Compound **8–PG***

A solution of **8** (23 mg, 0.04 mmol) and **PG–Tos** (100 mg) in 5 mL of *N*,*N*-dimethylformamide (DMF) was stirred for 2 days at 70 °C. Salts were removed by filtration and volatiles were removed under reduced pressure. The remaining residue was triturated with toluene (3×10 mL), yielding an orange solid (50 mg). ^{1}H NMR (300 MHz, DMSO-d_6): δ=2.29 (s, 9H, Tos–CH_3), 3.34 (br, 31H, polyether), 3.63 (s, 4H, C–CH_2), 3.70 (s, 8H, N–CH_2), 7.10 (m, 6H, 2×aromatic H–tosyl), 7.26 (m, 4H, pyridyl), 7.48 (dd, 6H, ^1J=8.1 Hz, ^2J=1.8 Hz, 2H, tosyl aromatic), 7.58 (d, 4H, J=7.8 Hz, pyridyl), 7.75 (m, 6H, PTE aromatic and pyridyl), 8.49 (dd, 4H, ^1J=2.4 Hz, ^2J=0.9 Hz, pyridyl). ^{13}C NMR (75.4 MHz, DMSO-d_6):=21.3, 21.5, 58.2, 59.6, 122.6, 122.7, 125.8, 126.0, 128.5, 128.7, 128.9, 129.4, 137.0, 138.0, 146.3, 149.3, 159.7.

*4.2.6. Compound **7–PG***

A solution of **7** (60 mg, 0.1 mmol) and **PG–Tos** (260 mg) in 5 mL DMF was stirred for 2 days at 70 °C. After cooling to room temperature, a precipitate was removed by filtration and DMF was removed under reduced pressure. The residue was triturated with toluene (3×10 mL), yielding a yellow solid (90 mg). ^{1}H NMR (300 MHz, DMSO-d_6): δ=2.29 (s, 12H, Tos–CH_3), 3.34–3.83 (52H, PG overlapping C–CH_2 and N–CH_2), 7.10 (m, 8H), 7.35 (m, 4H, pyridyl), 7.48 (m, 11H, 2×aromatic H–tosyl), 7.67–7.82 (m, 9H), 8.49 (br, 4H, pyridyl). ^{13}C NMR (75.4 MHz, DMSO-d_6): δ=21.2, 54.5, 59.3, 122.3, 122.4, 122.7, 123.1, 125.0, 128.5, 137.2, 138.0, 146.3, 149.2, 149.2, 159.0.

4.3. Preparation of metal complexes

*4.3.1. For Co_2–**7–PG** and Co_2–**8–PG***

A solution of **7–PG** or **8–PG** containing 1 mmol of ligand unit was dissolved in 9.8 mL of methanol and 0.2 mL of 0.1 mmol $CoSO_4 \cdot 7H_2O$ was added into it. Solution was stirred overnight. Further methanol was removed under reduced pressure. HEPES buffer (10 mL, 0.1 M) was added into it in order to make 1 mmol Co_2–**7–PG** and Co_2–**8–PG** solution, which is further used for hydrolysis titrations.

*4.3.2. For Zn_2–**7–PG** and Zn_2–**8–PG***

A solution of **7–PG** or **8–PG** containing 1.5 mmol of ligand unit and 3 mmol of $Zn(ClO_4)_2 \cdot 6H_2O$ was dissolved in 10 mL of 0.1 M HEPES buffer to make 1.5 mmol Zn_2–**7–PG** and Zn_2–**8–PG** solution which was further used for TEM experiment and the indicator displacement assay. For TEM experiments, Zn_2–**8–PG** solution was removed under reduced pressure and solid residue was dispersed in the THF.

4.4. General spectroscopic methods

Absorption spectra were recorded on a Varian Cary 50 Bio UV–vis spectrophotometer. Samples for all absorbance spectra used 0.1 M *N*-2-hydroxyethylpiperazine-*N*′-2-ethanesulfonic acid (HEPES) buffer at pH 7.4 as solvent in Spectrosil quartz cuvettes having a path length of 1 cm. Indicator displacement assay protocols,[8] kinetic analyses,[44] and dissociation constant determinations (modified Benesi–Hildebrand method)[48] have been described previously. All absorption spectra for titrations and Benesi–Hildebrand plots used are provided in Supplementary data.

Acknowledgements

We thank the Clemson University Department of Chemistry and Center for Optical Materials Science and Engineering Technologies for support, and Amar Kumbhar for assistance with TEM.

Supplementary data

Additional experimental detail, NMR spectra, and spectra from titrations and displacement experiments. Supplementary data associated with this article can be found in the online version, at doi:10.1016/j.tet.2009.03.051.

References and notes

1. Croddy, E. *Jane's Intelligence Rev.* **1995**, *7*, 520–523.
2. Burnworth, M.; Rowan, S. J.; Weder, C. *Chem.—Eur. J.* **2007**, *13*, 7828–7836.
3. Royo, S.; Martínez-Máñez, R.; Sancenón, F.; Costero, A. M.; Parra, M.; Gil, S. *Chem. Commun.* **2007**, 4839–4847.
4. Yang, Y. C.; Baker, J. A.; Ward, J. R. *Chem. Rev.* **1992**, *92*, 1729–1743.
5. Yang, Y. C. *Acc. Chem. Res.* **1999**, *32*, 109–115.
6. Weston, J. *Chem. Rev.* **2005**, *105*, 2151–2174.
7. Benning, M. M.; Shim, H.; Raushel, F. M.; Holden, H. M. *Biochemistry* **2001**, *40*, 2712–2722.
8. Morgan, B. P.; He, S.; Smith, R. C. *Inorg. Chem.* **2007**, *46*, 9262–9266.
9. Leevy, W. M.; Johnson, J. R.; Lakshmi, C.; Morris, J.; Marquez, M.; Smith, B. D. *Chem. Commun.* **2006**, 1595–1597.
10. Hanshaw, R. G.; Lakshmi, C.; Lambert, T. N.; Johnson, J. R.; Smith, B. D. *ChemBioChem* **2005**, *6*, 2214–2220.
11. Hanshaw, R. G.; Smith, B. D. *Bioorg. Med. Chem.* **2005**, *13*, 5035–5042.
12. Lee, H. N.; Swamy, K. M. K.; Kim, S. K.; Kwon, J. Y.; Kim, Y.; Kim, S. J.; Yoon, Y. J.; Yoon, J. *Org. Lett.* **2007**, *9*, 243–246.
13. Jang, Y. J.; Jun, E. J.; Lee, Y. J.; Kim, Y. S.; Kim, J. S.; Yoon, J. *J. Org. Chem.* **2005**, *70*, 9603–9606.
14. Shiraishi, H.; Jikido, R.; Matsufuji, K.; Nakanishi, T.; Shiga, T.; Ohba, M.; Sakai, K.; Kitagawa, H.; Okawa, H. *Bull. Chem. Soc. Jpn.* **2005**, *78*, 1072–1076.
15. Matsufuji, K.; Shiraishi, H.; Miyasato, Y.; Shiga, T.; Ohba, M.; Yokoyama, T.; Okawa, H. *Bull. Chem. Soc. Jpn.* **2005**, *78*, 851–858.
16. Adams, H.; Bradshaw, D.; Fenton, D. E. *Inorg. Chim. Acta* **2002**, *332*, 195–200.
17. O'Neil, E. J.; Smith, B. D. *Coord. Chem. Rev.* **2006**, *250*, 3068–3080.
18. Leevy, W. M.; Gammon, S. T.; Jiang, H.; Johnson, J. R.; Maxwell, D. J.; Jackson, E. N.; Marquez, M.; Piwnica-Worms, D.; Smith, B. D. *J. Am. Chem. Soc.* **2006**, *128*, 16476–16477.
19. Nguyen, B. T.; Anslyn, E. V. *Coord. Chem. Rev.* **2006**, *250*, 3118–3127.
20. Knapton, D.; Burnworth, M.; Rowan, S. J.; Weder, C. *Angew. Chem., Int. Ed.* **2006**, *45*, 5825–5829.
21. He, S.; Iacono, S. T.; Budy, S. M.; Dennis, A. E.; Smith, D. W.; Smith, R. C. *J. Mater. Chem.* **2008**, *18*, 1970–1976.
22. LeJeune, K. E.; Wild, J. R.; Russell, A. J. *Nature (London)* **1998**, *395*, 27–28.
23. Lejeune, K. E.; Mesiano, A. J.; Bower, S. B.; Grimsley, J. K.; Wild, J. R.; Russell, A. J. *Biotechnol. Bioeng.* **1997**, *54*, 105–114.
24. Hovestad, N. J.; Eggeling, E. B.; Heidbuchel, H. J.; Jastrzebski, J. T. B. H.; Kragl, U.; Keim, W.; Vogt, D.; Van Koten, G. *Angew. Chem., Int. Ed.* **1999**, *38*, 1655–1658.
25. Bosman, A. W.; Janssen, H. M.; Meijer, E. W. *Chem. Rev.* **1999**, *99*, 1665–1688.
26. Gorman, C. *Adv. Mater.* **1998**, *10*, 295–309.
27. Zeng, F.; Zimmerman, S. C. *Chem. Rev.* **1997**, *97*, 1681–1712.
28. Tomalia, D. A.; Durst, H. D. *Top. Curr. Chem.* **1993**, *165*, 193–313.
29. Sunder, A.; Heinemann, J.; Frey, H. *Chem.—Eur. J.* **2000**, *6*, 2499–2506.
30. Huck, W. T. S.; Snellink-Ruel, B. H. M.; Lichtenbelt, J. W. T.; van Veggel, F. C. J. M.; Reinhoudt, D. N. *Chem. Commun.* **1997**, 9–10.
31. Teta, N. L.; Brown, D.; Glass, M. (Technical Solutions Group International, USA). U.S. Patent 6,913,928 B2, 2005.
32. Tao, K. W. C.; Yu, P.; Roberts, R. L. (Shaklee Corporation, USA). PCT Int. Appl. 2003013566, 2003; 36 pp.
33. Patel, M. V.; Chen, F.-J. (Lipocine, Inc., USA). PCT Int. Appl. 2000050007, 2000; 98 pp.
34. Akiyama, Y.; Nagahara, N.; Kitano, M.; Nakao, M. (Takeda Chemical Industries, Ltd., Japan). PCT Int. Appl. 9842311, 1998; 55 pp.
35. Guillou, V.; Morancais, J.-L. (L'Oreal, Fr.). Eur. Pat. Appl. 1166747, 2002; 11 pp.
36. Valenty, V. B. (VB Cosmetics Inc., USA). U.S. 5747018, 1998; 7 pp. Cont.-in-part of U.S. Ser. No. 415,143, abandoned.
37. Cain, F. W.; McNeill, G. P.; Tongue, T. (Unilever N.V., Neth.; Unilever PLC). Eur. Pat. Appl. 1249180, 2002; 9 pp.
38. Vulfson, E. N.; Law, B. A. (Nutrahealth Ltd. (UK), UK). PCT Int. Appl. 2000041491, 2000; 91 pp.
39. Sunder, A.; Mulhaupt, R. (Bayer Aktiengesellschaft, Germany). 99-EP9773 2000037532, 2000; 13 pp.
40. Stiriba, S. E.; Slagt, M. Q.; Kautz, H.; Gebbink, R. J. M. K.; Thomann, R.; Frey, H.; Van Koten, G. *Chem.—Eur. J.* **2004**, *10*, 1267–1273.
41. Slagt, M. Q.; Stiriba, S. E.; Kautz, H.; Gebbink, R. J. M. K.; Frey, H.; Van Koten, G. *Organometallics* **2004**, *23*, 1525–1532.
42. Slagt, M. Q.; Stiriba, S. E.; Klein Gebbink, R. J. M.; Kautz, H.; Frey, H.; van Koten, G. *Macromolecules* **2002**, *35*, 5734–5737.
43. Breslow, R.; Singh, S. *Bioorg. Chem.* **1988**, *16*, 408–417.
44. Seo, J. S.; Sung, N. D.; Hynes, R. C.; Chin, J. *Inorg. Chem.* **1996**, *35*, 7472–7473.
45. Kirby, A. J.; Jencks, W. P. *J. Am. Chem. Soc.* **1965**, *87*, 3209–3216.
46. Fabbrizzi, L.; Marcotte, N.; Stomeo, F.; Taglietti, A. *Angew. Chem., Int. Ed.* **2002**, *41*, 3811–3814.
47. Kurz, K.; Gobel, M. W. *Helv. Chim. Acta* **1996**, *79*, 1967–1979.
48. Hammond, P. R. *J. Chem. Soc.* **1964**, 479–484.